Iran J Sci Technol Trans Sci (2022) 46:1045–1054
https://doi.org/10.1007/s40995-022-01299-1

RESEARCH PAPER

A Study on Electrical Properties of Nanofiber Composites: Effects of PCL/AgNO3/ZnO Concentration Percentages

Unal Kurt[1] · Selcuk Atis[2] · Zuhal Polat[2] · Mehmet Tektas[3] · Umit K. Terzi[2]

Received: 20 June 2021 / Accepted: 21 March 2022 / Published online: 31 May 2022

Abstract
Nanofibers with multifunctional properties hold great promise as they allow components for a wide range of medical applications. In this study, zinc oxide, silver nitrate and Polycaprolactone were used in the production of nanofiber composite material by coaxial electrospinning process. PCL concentrations of 5, 10, and 15% by weight were utilized in all of the samples, and different amounts of silver nitrate and zinc oxide were used. Functional groups of silver nitrate, zinc oxide, and Polycaprolactone materials were determined by Fourier transform infrared spectroscopy. Morphological analyzes were carried out with scanning electron microscopy. For all solutions, before coaxial electrospinning, physical properties such as density, liquid state ac conductivity, and viscosity were measured. For the 20 Hz–3 MHz frequency range, after coaxial electrospinning, D-factors and capacitance of nanofiber composite materials were measured and dielectric loss, permittivity, and the solid-state alternating current conductivity were calculated for all solutions. The effects of silver nitrate, zinc oxide, and Polycaprolactone concentration percentages on the solid-state ac conductivity and the dielectric constant were analyzed and comparisons were made with the results obtained.

Keywords Electrospinning · Nanomaterials · Biocomposites · Electrical properties

1 Introduction

With the rapid improvement in nanotechnology over the last two decades, significant progress was made not only in the fabrication and measurement of nanostructures but also for their functional purposes. As a crucial one-dimensional nanostructure, nanofibers have a particularly very high specific surface area and therefore nanofiber membranes are very porous with superb pore interconnectivity. According to the literature, it can be easily seen that the electrospinning process has been reported for nanofiber production for different purposes. Electrospinning is a basic and versatile process for the production of polymer, ceramic, and composite fiber. Nanofibers polymer materials fabricated by electrospinning have obtained immense research interest because of their functional properties, such as high surface-area-to-volume and aspect ratios. There are some alternative operation types of electrospinning. One of them is coaxial needle electrospinning. The biomedical engineering applications, method details, and principles of coaxial-needle electrospinning have been stated in detail in the literature (Komur et al. 2017).

This coaxial electrospinning (CAE) process has attracted great interest from researchers because of its novel molecular structure and remarkable electronic properties and its promising applications in photosensitizers, gas sensor devices, stabilizers as functional materials and biochemistry and biomedical engineering applications. Although several research papers have been published in recent years, CAE processing is a relatively new technique but there are many applications in this technique that need to be researched. Drug delivery, tissue engineering and biomedical applications are the applications CAE gains importance and takes place (Cesur et al. 2020; Croitoru et al. 2021; Saatcioglu et al. 2021). the Among various types of biomaterials, Polycaprolactone (PCL) has many

✉ Selcuk Atis
satis@marmara.edu.tr

[1] Amasya University, Amasya, Turkey

[2] Marmara University, Goztepe Campus, 34722 Istanbul, Turkey

[3] Bandırma Onyedi Eylul University, Bandırma, Turkey

advantages such as biocompatibility, biodegradability, low cost, and ease of control for fabricating process in electrospinning (Paneva et al. 2011; Hou et al. 2002). Zinc oxide (ZnO) a wurtzite n-type semiconductor, which is in its varying forms with unique properties, such as direct bandgap (3.37 eV), the high exciton binding energy (60 meV), and good resistivity (10−3 to 105 Ωcm) is among the widely explored functional metal oxide semiconductors (Patil et al. 2015). Virovska et al. have shown that Electrospun poly(lactic acid) (PLA) was surface-functionalized with nanosized ZnO leading to nonwoven mats in which ZnO was coated either on the surface or within the bulk, the former exhibiting higher photocatalytic activity (Virovska et al. 2014). Dobrzański et al. have stated that $AgNO_3$ leads to the higher electrical conductivity of the solution along with the increasing fraction of silver nitrate additives relative to the initial solution. They also showed that the fraction of silver nitrate affects the surface area of the nanofibers obtained (Dobrzański et al. 2014). Functional polymer nanocomposites can meet these requirements and the use of various conductive precursors, such as metallic, ceramic, nanoparticles, thin films and nanofibers, have been significantly explored and revealed to improve the conductivity and dielectric properties. However, insufficient research has been done on the dielectric properties of the composites enhanced by these nanocomposites.

By using dielectric spectroscopies, Kaya et al. examined the mixing temperatures' effects on dielectric properties of poly(methyl methacrylate) (PMMA)-pristine bentonite nanocomposites. They observed that the permittivity decreases and the dielectric relaxation displaces toward the lower frequencies by lowering the mixing temperature (Uğur Kaya et al. 2014). Kaya et al. investigated the dielectric and electric properties of Poly(vinyl imidazole)–Na–Bentonite composite. Conductivity was increased at 25 °C according to the studies done on the current and voltage. From the capacitive measurements it can be concluded that the samples show typical dielectric behavior. Depending on maximum interactions at 25 °C, loss factors and alternating current conductivity are also high (Kaya et al. 2011). Beside those of work composites are used in a variety of different fields for different purposes (Parlar et al. 2019; Kayiran 2022; Singh et al. 2020; Akkurt et al. 2021).

In this work, the goal is to analyze the effects of concentration percentages of PCL and $AgNO_3$ on the electrical properties of PCL/$AgNO_3$/ZnO nanofiber composites produced by using CAE processing. To observe the effects of concentration percentages of PCL and $AgNO_3$ on electrical properties of nanofiber composites, nine different samples were prepared with three different concentration percentages and dielectric spectroscopy was used to obtain information about interactions. The behavior of a dielectric can be studied through the real part (ε') and the imaginary part (ε'') of the dielectric constant and behavior of conductivity (σ^*) can also be studied through the real part (σ') and the imaginary part (σ'') of the alternating current conductivity.

2 Materials and Methods

2.1 Preparation of PCL/$AgNO_3$/ZnO Composite Solutions

Polycaprolactone (PCL) was selected as a biopolymer material and bought from Sigma-Aldrich. PCL's average molecular weight (M_w) was 80 kg/mol. No extra purification or treatment was carried out for the use of PCL. A solution of PCL was produced with various concentrations and the percentages of solution concentration were 5, 10 and 15 wt.%. PCL was dissolved in Dimethylformamide (DMF) and Tetrahydrofuran (THF) mixture with a constant w/w 1:1 ratio and a magnetic stirrer stirred all of these solutions at 40 °C for 2 h. The purity of the THF and DMF is 99%. $AgNO_3$ and ZnO are selected as dielectric property agents. ZnO was also bought from Sigma-Aldrich and its average molecular weight was 81.37 g/mol. $AgNO_3$ was purchased from Merck and the average molecular weight of $AgNO_3$ was 168.87 g/mol. The percentages of $AgNO_3$ solution concentrations were 0.5 wt.%, 1 wt.% and 2 wt.% and the percentages of ZnO solution concentration were 5 wt.%. ZnO and $AgNO_3$ were dissolved in DMF and THF mixture with a constant ratio of w/w 1:1 and the magnetic stirrer stirred all of these solutions at 40 °C for 3 h.

2.2 Coaxial Electrospinning of PCL/$AgNO_3$/ZnO Composite Nanofibers

Samples were prepared in different concentrations using polymer and dielectric properties agent solutions and detailed information about the contents of the nine samples have been listed in Table 1 and also supported with coaxial electrospinning parameters.

As can be seen in the schematic design given in Fig. 1, the solutions of PCL, ZnO and $AgNO_3$ were placed in three different plastic syringes and pinhead connected to a high voltage generator with the coaxial needle. Coaxial electrospinning was successfully carried out and PCL/$AgNO_3$/ZnO multilayered nanocomposite fibers were synthesized.

Table 1 The solution properties of nine samples and sample codes for each different polymer concentration

Sample no	Material compositions	Feeding speed (ml/h)	Distance between collector and needle (cm)	Applied voltage (kV)	Humidity (g/m^3)	Temperature (°C)
S1	PCL (5 wt.%)	0.01	9	25.9	58.3	26.9
	$AgNO_3$ (0.5 wt.%)	0.01				
	ZnO (5 wt.%)	0.01				
S2	PCL (5 wt.%)	0.01	9	21.8	63.8	24.3
	$AgNO_3$ (1 wt.%)	0.01				
	ZnO (5 wt.%)	0.01				
S3	PCL (5 wt.%)	0.02	9	23.3	60.4	27.3
	$AgNO_3$ (2wt.%)	0.02				
	ZnO (5 wt.%)	0.02				
S4	PCL (10 wt.%)	0.02	9	20.1	60	26.7
	$AgNO_3$ (0.5 wt.%)	0.01				
	ZnO (5 wt.%)	0.01				
S5	PCL (10 wt.%)	0.02	9	23.3	63.8	27.3
	$AgNO_3$ (1 wt.%)	0.02				
	ZnO (5 wt.%)	0.02				
S6	PCL (10 wt.%)	0.02	9	18.4	60	26.7
	$AgNO_3$ (2 wt.%)	0.01				
	ZnO (5 wt.%)	0.01				
S7	PCL (15 wt.%)	0.04	9	18.6	60	26.7
	$AgNO_3$ (0.5 wt.%)	0.04				
	ZnO (5 wt.%)	0.04				
S8	PCL (15 wt.%)	0.04	9	21.7	60	24.6
	$AgNO_3$ (1 wt.%)	0.04				
	ZnO (5 wt.%)	0.04				
S9	PCL (15 wt.%)	0.05	9	21.8	50.5	27.3
	$AgNO_3$ (2 wt.%)	0.05				
	ZnO (5 wt.%)	0.05				

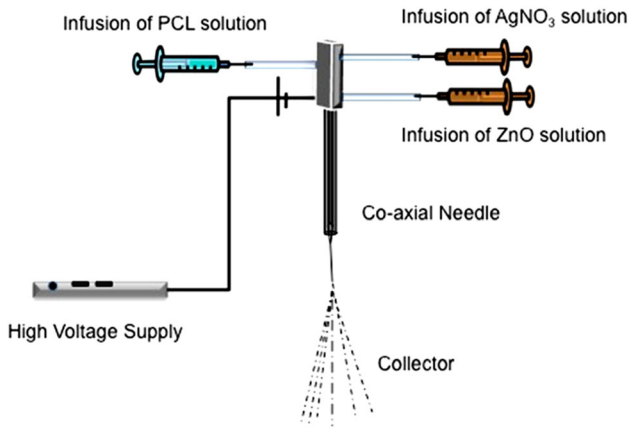

Fig. 1 Schematic design of the experimental setup for coaxial electrospinning method

2.3 Characterization

2.3.1 Physical Properties of PCL, $AgNO_3$ and ZnO Solutions

Physical properties of PCL, $AgNO_3$ and ZnO solutions are studied in two sections as liquid state ac conductivity, density and viscosity and solid-state ac conductivity, permittivity and dielectric loss.

2.3.1.1 Liquid State ac Conductivity, Density and Viscosity Physical properties of PCL (5, 10 and 15 wt.%), $AgNO_3$ (0.5, 1 and 2 wt.%) and ZnO (5 wt.%) solutions were determined. THF and DMF were used together to dissolve PCL, $AgNO_3$ and ZnO. All these samples' viscosities were measured by a viscometer (Lamy Rheology Instruments B-one Touch Viscometer). Liquid state ac

conductivities of these solutions were measured with a Cond 3110 (Set 1-2CA101, Germany). In Table 2, for each solution, measured viscosity, density and liquid state ac conductivity values are shown before preparing the nine different blend solutions. During the measurement tests, four different examples were processed and measured to figure out the average numbers of them.

2.3.1.2 Solid-State ac Conductivity (SSACC), Dielectric Loss and Permittivity For SSACC, dielectric loss and permittivity measurements, samples were cut in a square shape with a side length of 20 mm. 1 V_{rms} potential and at 23 °C temperature, electrical measurements of PCL (5, 10 and 15 wt.%), $AgNO_3$ (0.5, 1 and 2 wt.%) and ZnO (5 wt.%) solutions were completed by using Wayne Kerr 6500 B Precision Impedance Analyzer (20 Hz–5 MHz) and the SSACC, the dielectric loss and permittivity values were obtained by calculations. In Table 3, the average values over a range of frequency of 20 Hz–3 MHz for the dielectric loss, the permittivity and the real and imaginary parts of SSACC are given for each solution after preparing the nine different blends solutions.

2.3.2 Morphology of the Electrospun Nanocomposite Fibers (ENF)

Morphological analysis of the produced ENF was examined by an SEM (VEGA3 SB, Tescan USA). Before the analysis, samples were coated with gold for 5 min. By using Olympus AnalySIS 5 (Olympus, USA), image visualization software, diameter measurements of the electrospun nanocomposites materials were taken.

2.3.3 Fourier Transform Infrared Spectroscopy (FTIR)

For the determination of the functional groups of used materials, PerkinElmer FT-IR Spectrometer Spectrum Two was used. Tests were conducted at 23 °C room temperature for all ENF samples by running ten scans with a resolution of 4 cm^{-1} in the wavenumber range of 400–4000 cm^{-1}.

3 Results and Discussion

3.1 Morphological Characterization

Unique PCL/$AgNO_3$/ZnO ENFs were produced to examine their capacity for new functional opportunities with the advantage of low cost, biomedical applications and nanocomposites. Fiber diameter, bead structures, and porosity are important morphological features, and every one of them can find a different application area in healthcare engineering applications. SEM images, fiber diameter range graphics and average fiber diameter for each sample are showed in Fig. 2. ZnO nanoparticles were observed in the PCL nanofibers in the samples. All the fabricated nanocomposite materials showed uniform fiber diameter distribution as shown in Fig. 2a, b. It has been shown that the diameter of nanocomposite fibers will decrease to a large extent with the increasing concentration of silver nitrate nanoparticles in nanocomposite materials (Augustine et al. 2016a). Average fiber diameters were 559.66 nm as seen in Fig. 2c for all of the samples (S1 to S9).

3.2 Fourier Transform Infrared Spectroscopy (FTIR)

For the chemical bond analysis of PCL/AgNO3/ZnO ENF samples (S1 to S9), FTIR analyses were carried out. In FTIR analysis, it is expected that a nanocomposite material reflects the characteristic peaks of its components.

The infrared spectrum bands for 5 wt.% PCL/1 wt.% $AgNO_3$/5 wt.% ZnO nanocomposite sample in the wavenumber range of 4000 to 450 cm^{-1} can be seen in Fig. 3. In all composite samples, characteristic peaks of PCL were observed including asymmetric CH_2 stretching at 2944 cm^{-1}, asymmetric strong bands of carbonyl stretching mode approximately 1722 cm^{-1}, symmetric CH_2 stretching at 2866 cm^{-1}, asymmetric COC stretching, C–O and C–C stretching in the crystalline phase at 1293 cm^{-1}, OC–C stretching at 1168 cm^{-1}, C–O and C–C stretching in the amorphous phase at 1046 cm^{-1}, and finally symmetric COC stretching at 1107 cm^{-1}

Table 2 Measured liquid state ac conductivity, density and viscosity values for different concentrations of PCL, ZnO and $AgNO_3$ solutions before preparing the nine different blend solutions

Solution concentrations	Viscosity (mPas)	Liquid state ac conductivity (μS/cm)	Density (g/cm^3)
5 wt.%PCL	65.4	6.18	0.9525
10 wt.%PCL	120.8	0.86	0.9728
15 wt.%PCL	182.3	0.64	0.9975
5 wt.% ZnO	45.9	3.2	0.9828
0.5 wt.% $AgNO_3$	10.1	249	0.9496
1 wt.% $AgNO_3$	10.2	457	0.9516
2 wt.% $AgNO_3$	10.5	936	0.9554

Table 3 The average values over a range of frequency of 20 Hz–3 MHz for the permittivity, the dielectric loss and the real and imaginary parts of SSACC for each sample

Sample no	wt.%PCL	wt.%ZnO	wt.%$AgNO_3$	Average ε'	Average ε''	Average σ' (S/m)	Average σ'' (S/m)
S1	5	5	0.5	1.85E+00	4.37E−03	8.33E−08	2.72E−05
S2	5	5	1	2.74E−01	4.83E−04	1.09E−08	4.02E−06
S3	5	5	2	9.71E−01	2.56E−03	4.25E−08	1.43E−05
S4	10	5	0.5	7.36E−01	1.75E−03	3.12E−08	1.08E−05
S5	10	5	1	3.43E−01	7.25E−04	1.37E−08	5.04E−06
S6	10	5	2	7.78E−01	1.71E−03	3.29E−08	1.14E−05
S7	15	5	0.5	5.58E+00	1.42E−02	2.47E−07	8.20E−05
S8	15	5	1	6.49E−01	1.53E−03	2.62E−08	9.53E−06
S9	15	5	2	6.45E−01	1.52E−03	2.76E−08	9.48E−06

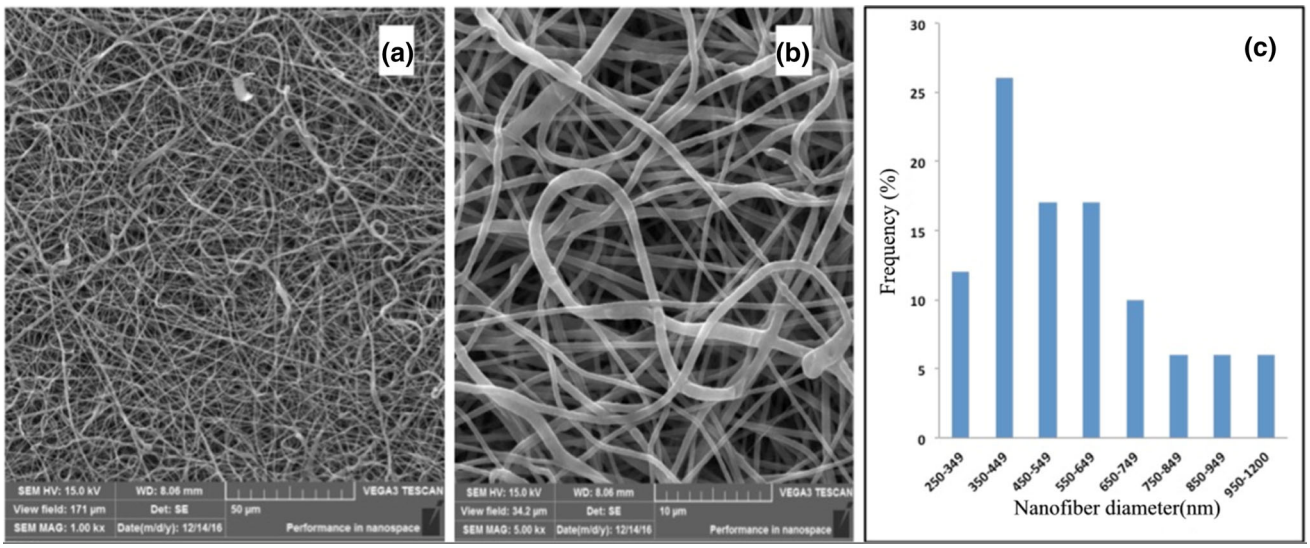

Fig. 2 Scanning electron microscopy (SEM) images of the 5 wt.% PCL/1 wt.% $AgNO_3$/5 wt.% ZnO nanocomposite fiber materials with fiber diameter frequency graphics. **a** Low magnification (× 1000), **b** high magnification (× 5000) and **c** diameter distributions of nanofiber compositions

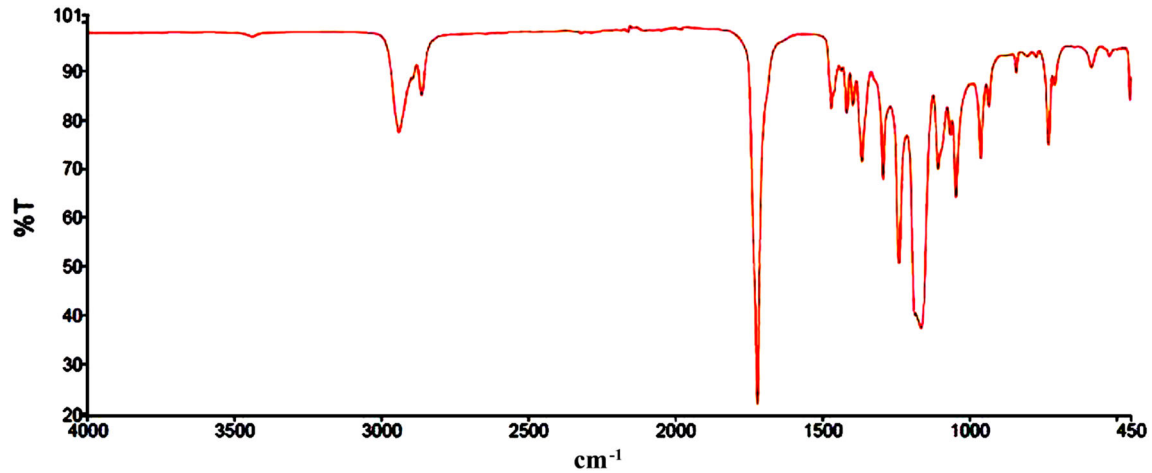

Fig. 3 FTIR Spectrum of the 5 wt.%PCL/1 wt.% $AgNO_3$/5 wt.% ZnO electrospun nanocomposite material

(Augustine et al. 2016b). Peaks of vibration which indicate ZnO come in view as C–H stretching at 2944 cm^{-1}, strong absorption peaks were observed at 1635 and 1631 cm^{-1}, which indicates the N–H band. 1418 and 1470 cm^{-1} were assigned to C–C stretching in an aromatic group. The narrow peaks at 1065 cm^{-1} and 1046 cm^{-1} were assigned to C–N stretching in aliphatic amines. The weak absorption bands at 453 cm^{-1} indicate Zn–O stretching. The region between 400 and 600 cm^{-1} corresponds to metal oxide (Elumalai et al. 2015). $AgNO_3$ showed peaks at 1651.4, 1542, 1396 and 1057 cm^{-1}. The bands obtained at 1396 and 1046 cm^{-1} are due to the presence of C-N stretching vibrations of aromatic and aliphatic amines. Molecules containing NO_2 groups, such as nitro compounds, nitrates, and nitramines, commonly exhibit asymmetric and symmetric stretching vibrations of the NO_2 group at the 1660 to 1500 cm^{-1} and 1390 to 1260 cm^{-1} region (Raheman et al. 2011).

3.3 Dielectric and Conductivity Studies

Dielectric behavior is studied through the real (ε') and imaginary (ε'') parts of the dielectric constant ($\varepsilon^* = \varepsilon' + j\varepsilon''$). ε' ε' is related to energy which is deposited by the external field and ε'' is related to energy loss (Uğur Kaya et al. 2014; Kaya et al. 2011);

$$\varepsilon' = C_p/C_0, \varepsilon'' = \varepsilon' \tan\delta \quad (1)$$

C_0 is the vacuum capacitance and calculated by;

$$C_0 = \varepsilon_0 \cdot A/d \quad (2)$$

where A is the area of the plates, ε_0, which equals 8.85×10^{12} F/m, is the electrical permittivity of a vacuum, d is the vertical span between the plates of the capacitance fixture.

AC conductivity (σ^*) was figured out by;

$$\sigma*(\omega) = \sigma' + j\sigma'' = \omega\varepsilon_0\varepsilon'' + j\omega\varepsilon_0\varepsilon' \quad (3)$$

where ε_0 is the free space dielectric constant, ω is angular frequency (Aydogdu et al. 2018; Kuru 2021).

As mentioned in Sect. 2.3.1.2, electrical measurements were completed by using Impedance Analyzer, at room temperature (23 °C) at 1 V_{rms} potential over a range of frequencies of 20 Hz to 3 MHz. To record the capacitance and tanδ data, the same procedure was repeated for each sample. First, by using Eq. 2, C_0 for each sample was calculated by using thickness, area, capacitance and tanδ data of each sample for 20 Hz–3 MHz frequency range. After calculation of the C_0 of each sample, the calculations of ε', ε'', σ' and σ'' were done by using Eqs. 1 and 3, respectively. After that average value calculations over a range of frequency of 20 Hz–3 MHz were done for ε', ε'', σ' and σ'' for each sample and values obtained from these procedures were presented in Table 3.

By using the data given in Table 3, graphs of average values of ε', ε'', σ' and σ'' for each sample were drawn and can be seen in Figs. 4, 5, 6, and 7, respectively.

In Fig. 4, change of average values of the real part of permittivity for nine different blend solutions can be seen via the concentration percentage of AgNO3. Figure 4, for each PCL (5, 10 and 15 wt.%), makes it possible to analyze the change of average values of the real part of permittivity by the increase of the concentration percentage of AgNO3.

In Fig. 5, change of average values of the imaginary part of permittivity for nine different blend solutions can be seen via the concentration percentage of AgNO3. Figure 5, for each PCL (5, 10 and 15 wt.%), makes it possible to analyze the change of average values of the imaginary part of permittivity by the increase of the concentration percentage of AgNO3.

In Fig. 6, change of the average values of the real part of the alternating current conductivity for nine different blend solutions can be seen via the concentration percentage of AgNO3. Figure 6, for each PCL (5, 10 and 15 wt.%), makes it possible to analyze the change of the average values of the real part of the alternating current conductivity by the increase of the concentration percentage of AgNO3.

In Fig. 7, change of the imaginary values of the real part of the alternating current conductivity for nine different blend solutions can be seen via the concentration percentage of AgNO3. Figure 7, for each PCL (5, 10 and 15 wt.%), makes it possible to analyze the change of the average values of the imaginary part of the alternating current conductivity by the increase of the concentration percentage of AgNO3.

For making the effects of concentration percentages of PCL and $AgNO_3$ on dielectric properties of the nanofiber composites produced by using coaxial electrospinning clear, for each concentration percentage of $AgNO_3$, the average of absolute values of differences for each PCL (5, 10 and 15 wt.%) have been calculated. Values obtained from calculations can be seen in Table 4.

By using data given in Table 4, graphs of the average of absolute values of differences for PCL (5, 10 and 15 wt.%) vs. wt.%$AgNO_3$ have been drawn and can be seen in Fig. 8.

As can be seen in Fig. 8a, while the concentration percentage of $AgNO_3$ changes from 0.5 to 1%, the change in percentage of the average of absolute values of differences for the permittivity is − 92.26% and when the concentration percentage of $AgNO_3$ changes from 1 to 2%, the change in percentage of the average of absolute values of differences for the permittivity is − 13.01%. Similarly, as can be seen in Fig. 8b, while the concentration percentage

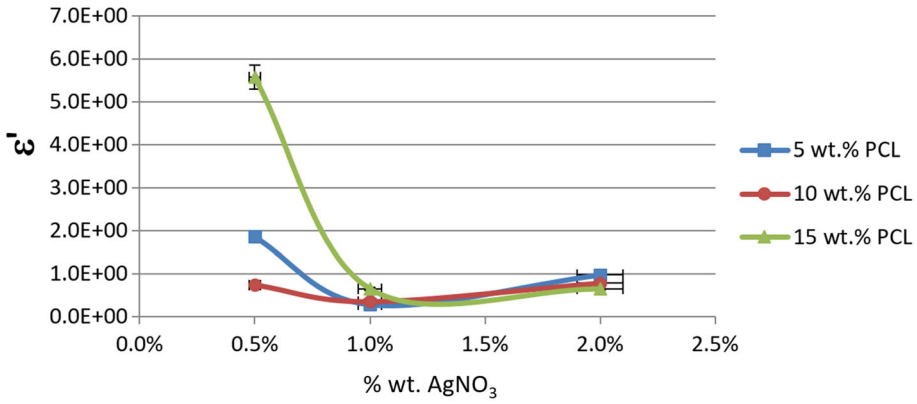

Fig. 4 Average values of the real part of permittivity for nine different blend solutions

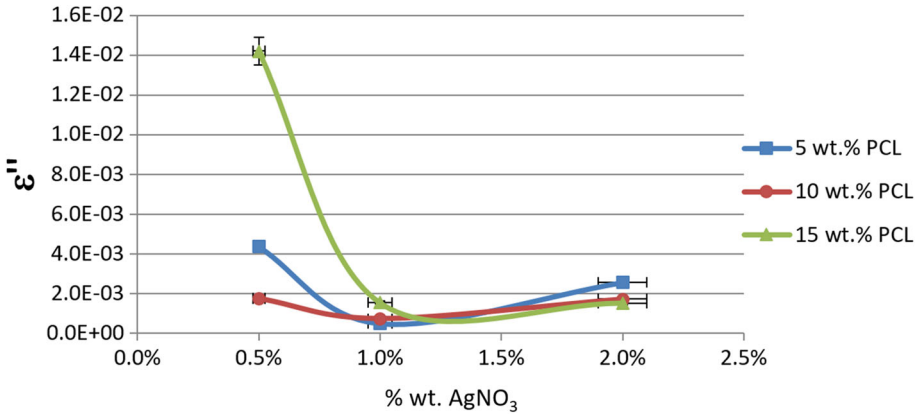

Fig. 5 Average values of the imaginary part of permittivity for nine different blend solutions

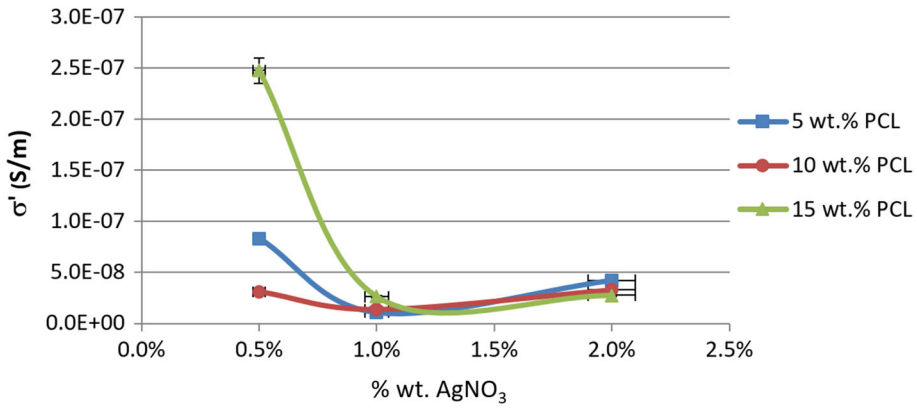

Fig. 6 Average values of the real part of the alternating current conductivity for nine different blend solutions

of $AgNO_3$ changes from 0.5 to 1%, the change in percentage of the average of absolute values of differences for the dielectric loss is − 91.56% and when the concentration percentage of $AgNO_3$ changes from 1 to 2%, the change in percentage of the average of absolute values of differences for the dielectric loss is − 0.97%.

The same situation is valid for the real part of ac conductivity and the imaginary part of ac conductivity. As can be seen in Fig. 8c, while the concentration percentage of $AgNO_3$ changes from 0.5 to 1%, the change in percentage of the average of absolute values of differences for the real part of the ac conductivity is − 92.93% and when the concentration percentage of $AgNO_3$ changes from 1 to 2%, the change in percentage of the average of absolute values of differences for the real part of the ac conductivity is − 3.06%. Similarly, as can be seen in Fig. 8d, while the concentration percentage of $AgNO_3$ changes from 0.5 to 1%, the change in percentage of the average of absolute values of differences for the imaginary part of the ac conductivity is − 92.26% and when the concentration percentage of $AgNO_3$ changes from 1 to 2%, the change in

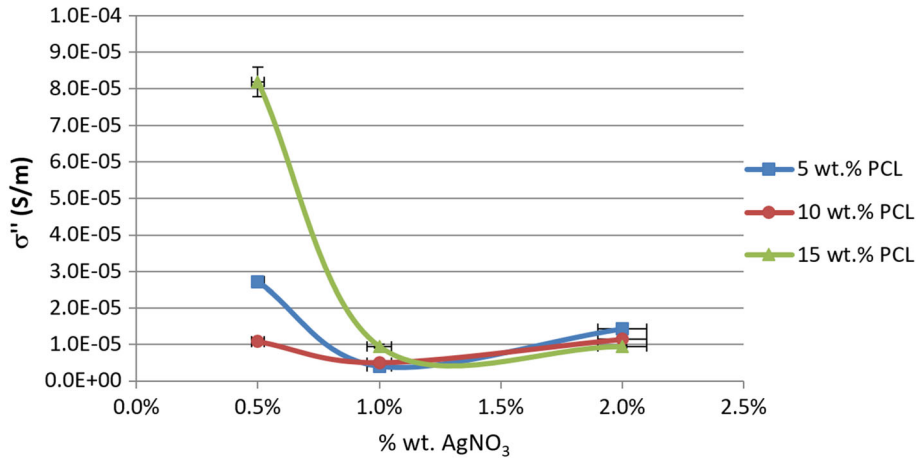

Fig. 7 Average values of the imaginary parts of the alternating current conductivity for nine different blend solutions

Table 4 Average of absolute values of differences for PCL (5, 10, and 15 wt.%) vs. wt.%$AgNO_3$

wt.%$AgNO_3$	Average of absolute values of differences for PCL (5, 10 and 15 wt.%)			
	ε'	ε''	σ' (S/m)	σ'' (S/m)
0.5	3.228448078	0.008297431	1.44194E−07	4.74548E−05
1.0	0.249881712	0.000700123	1.02001E−08	3.6723E−06
2.0	0.217367156	0.00069333	9.88801E−09	3.20041E−06

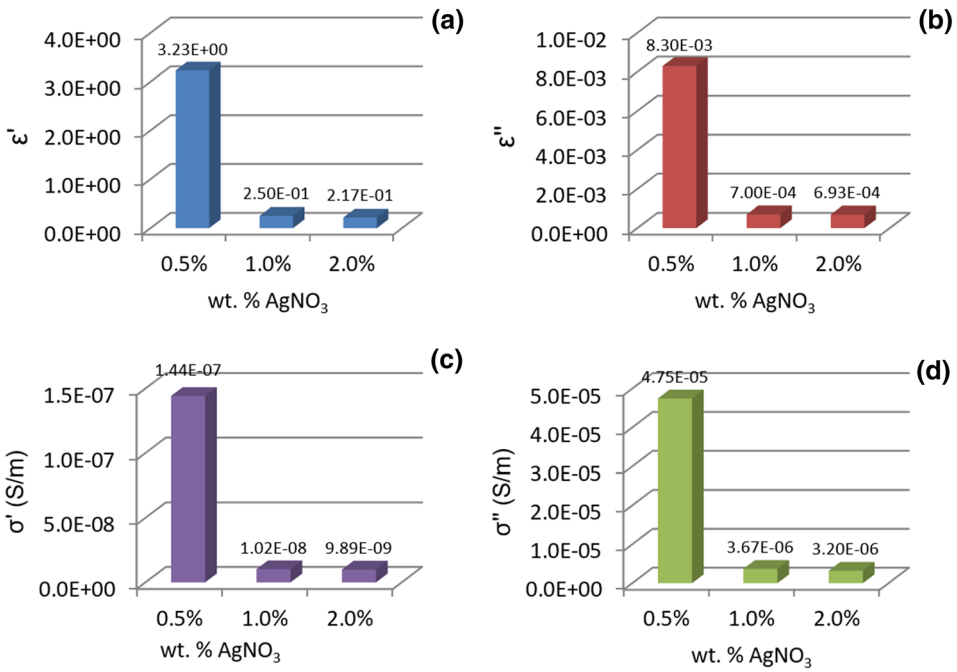

Fig. 8 The averages of absolute values of differences of **a** permittivity for PCL (5, 10 and 15 wt.%) for each concentration percentage of $AgNO_3$, **b** dielectric loss for PCL (5, 10 and 15 wt.%) for each concentration percentage of $AgNO_3$, **c** real part of alternating current conductivity for PCL (5, 10 and 15 wt.%) for each concentration percentage of $AgNO_3$, **d** imaginary part of alternating current conductivity for PCL (5, 10 and 15 wt.%) for each concentration percentage of $AgNO_3$

percentage of the average of absolute values of differences for the imaginary part of the ac conductivity is − 12.85%.

There is very little change in properties when either PCL or $AgNO_3$ are varied over the PCL range of 5–15% and the $AgNO_3$ range of 1–2%. From all the results explained above and Figs. 4, 5, 6 and 7, it clearly can be concluded that increasing the concentration percentage of $AgNO_3$ makes all the electrical properties studied in this paper almost independent from the concentration percentage of PCL.

4 Conclusion

Within this study, nine samples of nanocomposite material with fiber structure have been prepared by using Polycaprolactone (PCL), zinc oxide (ZnO) and silver nitrate ($AgNO_3$) and have been produced by a coaxial electrospinning method. Nine samples were examined under laboratory conditions and calculations were done by integrating the collected data to the equations presented in the theory. According to the results gathered, an increase in concentration percentage of $AgNO_3$ makes the variety of permittivity, dielectric loss and the real part and the imaginary part of ac conductivity of the studied samples almost PCL independent. In other words, adjusting the concentration percentage of $AgNO_3$ will be enough to vary the value of all the electrical properties of nanocomposite materials with the fiber structure studied in this paper. If these types of nanocomposite materials with fiber structure are going to be used for industrial purposes, it should be considered that the concentration percentage of $AgNO_3$ will play an important role to vary the value of permittivity, dielectric loss and the real part and the imaginary part of ac conductivity more than concentration percentage of PCL.

Acknowledgements The authors report no acknowledgement for this work.

Authors' contributions All authors read and approved the final version of the manuscript for publication.

Funding There is no funding for this work.

Availability of data and materials All raw data used in this manuscript are available and could be supplied upon request.

Declarations

Conflict of interest The authors declare that there is no conflict of interest.

References

Akkurt I, Malidarre RB, Kartal I, Gunoglu K (2021) Monte Carlo simulations study on gamma ray–neutron shielding characteristics for vinyl ester composites. Polym Compos. https://doi.org/10.1002/pc.26185

Augustine R, Kalarikkal N, Thomas S (2016a) Electrospun PCL membranes incorporated with biosynthesized silver nanoparticles as antibacterial wound dressings. Appl Nanosci 6(3):337–344

Augustine R, George SC, Kalarikkal N, Thomas S (2016b) Gentamicin loaded electrospun poly (ε-caprolactone)/TiO2 nanocomposite membranes with antibacterial property against methicillin resistant Staphylococcus aureus. Polym Plast Technol Eng 55(17):1785–1796

Aydogdu MO, Ekren N, Suleymanoglu M, Erdem-Kuruca S, Lin C-C, Bulbul E, Erdol MN, Oktar FN, Terzi UK, Kilic O (2018) Novel electrospun polycaprolactone/graphene oxide/Fe_3O_4 nanocomposites for biomedical applications. Colloids Surf B 172:718–727

Cesur S, Oktar FN, Ekren N, Kilic O, Alkaya DB, Seyhan SA, Ege ZR, Lin CC, Kuruca SE, Erdemir G, Gunduz O (2020) Preparation and characterization of electrospun polylactic acid/sodium alginate/orange oyster shell composite nanofiber for biomedical application. J Aust Ceram Soc 56(2):533–543

Croitoru A-M, Karaçelebi Y, Saatcioglu E, Altan E, Ulag S, Aydoğan HK, Sahin A, Motelica L, Oprea O, Tihauan B-M, Popescu R-C, Savu D, Trusca R, Ficai D, Gunduz O, Ficai A (2021) Electrically triggered drug delivery from novel electrospun poly(lactic acid)/graphene oxide/quercetin fibrous scaffolds for wound dressing applications. Pharmaceutics 13:957

Dobrzański L, Hudecki A, Chladek G, Król W, Mertas A (2014) Surface properties and antimicrobial activity of composite nanofibers of polycaprolactone with silver precipitations. Arch Mater Sci Eng 70(2):53–60

Elumalai K, Velmurugan S, Ravi S, Kathiravan V, Ashokkumar S (2015) Bio-fabrication of zinc oxide nanoparticles using leaf extract of curry leaf (*Murraya koenigii*) and its antimicrobial activities. Mater Sci Semicond Process 34:365–372

Hou Q, Grijpma DW, Feijen J (2002) Preparation of porous poly (ε-caprolactone) structures. Macromol Rapid Commun 23(4):247–252

Kaya AU, Esmer K, Tekin N, Beyaz SK (2011) Investigation of temperature, thermodynamic parameters and dielectrical properties of poly (vinylimidazole)–Na–bentonite nanocomposite. J Appl Polym Sci 120(2):874–879

Kayiran HF (2022) Numerical analysis of composite discs with carbon/epoxy and aramid/epoxy materials. Emerg Mater Res. https://doi.org/10.1680/jemmr.21.00052

Komur B, Bayrak F, Ekren N, Eroglu M, Oktar F, Sinirlioglu Z, Yucel S, Guler O, Gunduz O (2017) Starch/PCL composite nanofibers by co-axial electrospinning technique for biomedical applications. Biomed Eng Online 16(1):40

Kuru TŞ (2021) Frequency dependence of dielectric, conductivity, impedance and electrical modulus properties of La3+ substituted in cobalt-magnesium ferrites. J Inst Sci Technol 11(1):240–257

Paneva D, Manolova N, Argirova M, Rashkov I (2011) Antibacterial electrospun poly (ε-caprolactone)/ascorbyl palmitate nanofibrous materials. Int J Pharm 416(1):346–355

Parlar Z, Abdlhamed A, Akkurt İ (2019) Gamma-ray-shielding properties of composite materials made of recycled sport footwear. Int J Environ Sci Technol 16:5113–5116. https://doi.org/10.1007/s13762-018-1876-7

Patil PT, Anwane RS, Kondawar SB (2015) Development of electrospun polyaniline/ZnO composite nanofibers for LPG sensing. Procedia Mater Sci 10:195–204

Raheman F, Deshmukh S, Ingle A, Gade A, Rai M (2011) Silver nanoparticles: novel antimicrobial agent synthesized from an endophytic fungus Pestalotia sp. isolated from leaves of *Syzygium cumini* (L.). Nano Biomed Eng 3(3):174–178

Saatcioglu E, Ulag S, Sahin A, Yilmaz BK, Ekren N, Inan AT, Palaci Y, Ustundag CB, Gunduz O (2021) Design and fabrication of electrospun polycaprolactone/chitosan scaffolds for ligament regeneration. Eur Polym J 148:110357

Singh NB, Su C-H, Choa F-S, Arnold B, Cooper C, Cullum B, Kelly L (2020) Morphology and performance of organic nanocomposites for γ-ray sensing. Emerg Mater Res 9–2:520–526. https://doi.org/10.1680/jemmr.18.00050

Uğur Kaya A, Güner S, Esmer K (2014) Effects of solution mixing temperature on dielectric properties of PMMA/Pristine bentonite nanocomposites. J Appl Polym Sci 131(4):39907(1–7)

Virovska D, Paneva D, Manolova N, Rashkov I, Karashanova D (2014) Electrospinning/electrospraying vs electrospinning: a comparative study on the design of poly (l-lactide)/zinc oxide non-woven textile. Appl Surf Sci 311:842–850